Mitigation of Sub Synchronous Resonance in DFIG Based Windgeneration Using Fuzzy Logic Controller

Anjaneyulu Atkuri, M.Tech.,
PVP Siddhartha Institute of Technology,
Vijayawada, India.

A. PurnaChandrarao. ,
PVP Siddhartha Institute of Technology,
Vijayawada, India.

***Abstract*—The rapid growth of wind power systems worldwide will likely see the integration of large wind farms with electrical networks that are series compensated for ensuring stable transmission of bulk power. This may potentially lead to sub synchronous resonance (SSR) issues. Although SSR is a well-understood phenomenon that can be mitigated with flexible ac transmission system (FACTS) devices, scant information is available on the SSR problem in a series-compensated wind farm. This paper reports the potential occurrence and mitigation of SSR caused by an induction-generator (IG) effect as well as torsional interactions, in a series-compensated wind farm. In this study, a wind farm employing a self-excited induction generator is connected to the grid through a series-compensated line. The DFIG converters will be explored for SSR mitigation. The major contributions of the paper are 1) investigation of the potential of wind farm converters for SSR mitigation and 2) identification of an effective control signal for mitigating SSR using fuzzy logic controllers to simultaneously enhance both sub synchronous and super synchronous resonance modes .Extensive simulations have been carried out using Matlab/Simulink.**

***Keywords*— Doubly-Fed induction generator (DFIG), sub synchronous resonance (SSR), Fuzzy logic controller.**

I. INTRODUCTION

Sub synchronous resonance (SSR) phenomenon in wind farms connected with series compensated transmission network has been researched in recent literature [2]–[4]. It is well known that series compensation is an effective means of increasing power transfer capability of an existing transmission network. However, series compensation is shown to cause a highly detrimental phenomenon called sub synchronous resonance in electrical networks.

A grid side converter (GSC) of a DFIG has a similar topology of a STATCOM yet exchanges both active and reactive power in fast speed. Hence, the objective of this paper is to explore the control capability of DFIG-based wind farms in mitigating SSR using SSR damping controller at the GSC.

The unique feature of SSR phenomena in wind farms inter faced with series compensated network is that induction generator effect (IGE) due to the network resonant oscillatory model is the major cause of SSR. The frequency of torsional modes in wind turbines can be as low as 1–3 Hz. In order to have torsional interaction, the network mode should have a frequency of 57–59 Hz. This requires a very high level of series compensation which rarely happens. The rotor speed has been used in SSR mitigation control [2]-[4]. A preliminary study exploring the capability of the grid-side converters (GSCs) of a DFIG in mitigating SSR is presented in [11]. The control scheme is demonstrated to enhance the SSR damping. The line current and the voltage across the series compensation are chosen and their effectiveness will be discussed in the paper.

Therefore, the objective of the paper is twofold:

1) To investigate the potential of SSR mitigation in DFIG converters;

2) To identify a control signal for SSR mitigation and for overall system stabilization enhancement.

The paper is organized as follows. Section II presents the study system, the DFIG converter controls, and the auxiliary damping control for SSR mitigation. Section III presents Comparison of control input signals Section IV presents Fuzzy logic controller Section V presents the simulation results to demonstrate the effectiveness of the SSR damping controllers. Section VI concludes the paper.

II. STUDY SYSTEM AND SYSTEM MODEL

The study system based on the IEEE first benchmark model for SSR studies [12] is shown in Fig. 1, where a DFIG-based wind farm (100 MVA from the aggregation of 2-MW units) is connected to a 161-kV series-compensated line. The collective behavior of a group of wind turbines is represented by an equivalent lumped machine. This assumption is supported by several recent studies [13]–[16] that suggest that wind farm aggregation provides a reasonable approximation for system interconnection studies. In this paper, an aggregated DFIG model is used and the voltage level of the transmission network is chosen to be 161 kV. The machine and the network parameters are listed in the Appendix. The length of the transmission line is approximately 154 miles for which it is reasonable to install series compensation.

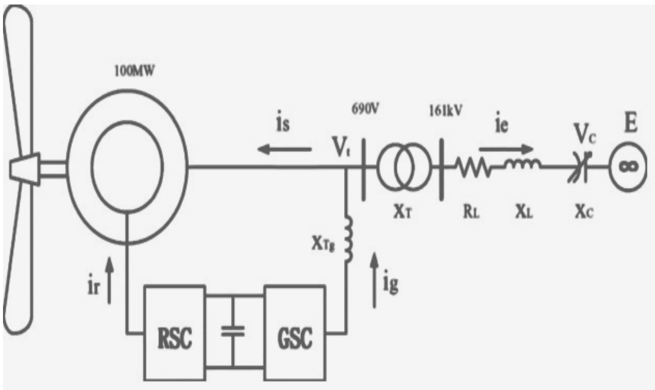

Fig.1 The study system. The rated power of the wind farm is 100 MVA. The nominal voltage of the wind farm terminal bus is 690 V and the nominal voltage of the network is 161 kV.

When individual wind turbines are aggregated, the aggregated inertia is scaled up. However, the base power is also scaled up; therefore, the per unit value of the inertia does not change. The same also happens to other machine parameters such as impedances. Therefore, the parameters of A 2-MW DFIG in per unit values can continue to be used for the equivalent wind generator.

As a summary, the complete dynamic system model includes the series compensated network model, the wind turbine aerodynamic model, the torsional dynamics model, the induction generator model, the dc-link model, and the DFIG's converter controls. The auxiliary SSR damping control will be designed and added in for SSR mitigation study.

2.1. DFIG Converter Controls:

Both rotor-side converter (RSC) and grid-side converter (GSC) controls are modeled in this study. Cascaded control loops similar to the ones in [17] are adopted in this paper. The control loops are shown in Figs. 2 and 3.

In the RSC control loops, the reference torque is obtained through the lookup table. When wind speed is greater than the rated speed, it is a constant value and is the optimal torque corresponding to the measured rotating speed. Through this lookup table, the wind turbine is able to extract the maximum wind power. The q -axis loop is to regulate the active power and the d-axis loop is to regulate the reactive power.

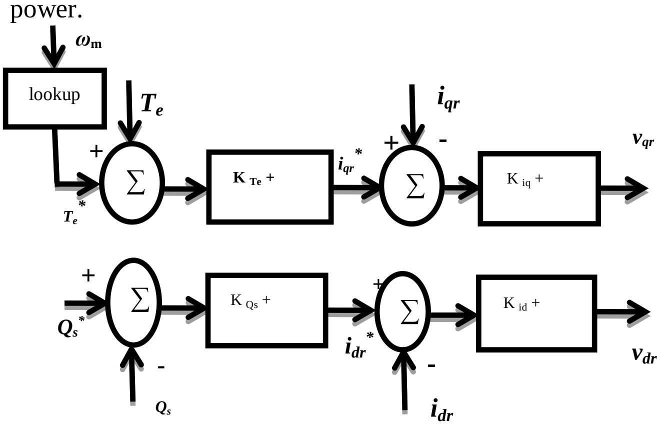

Fig 2. RSC control loops

In the GSC control loops, the q-axis loop is to regulate the dc-link voltage and the d-axis loop is to regulate the terminal voltage, as shown in Fig. 3.

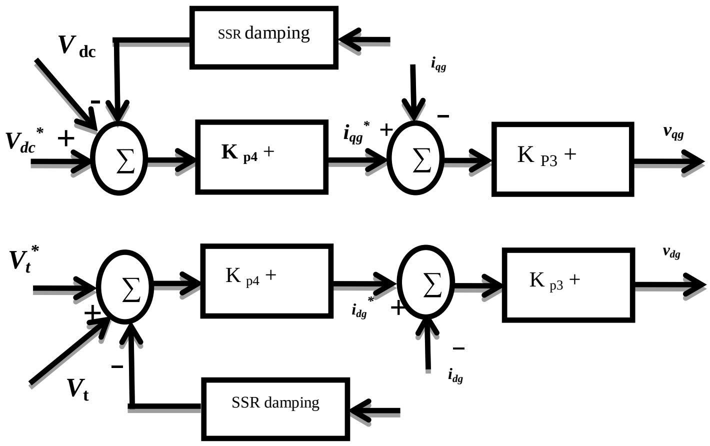

Fig.3 Supplementary control schemes in the GSC control loop for SSR mitigation through either the terminal voltage modulation or dc-link voltage modulation.

2.2. Auxiliary SSR Damping Control

It has been identified in [3] and [9] that the RSC control loop gains negatively impact the SSR network mode and these gains have to be limited. It is, therefore, not suitable to explore SSR mitigation through RSCs. Instead, the focus is on GSC. The GSC is similar to a STATCOM in terms of the topology. The difference between STATCOM and GSC SSR mitigation is the consequent impact. For example, a GSC is connected to an RSC through a dc-link. Hence, SSR mitigation in GSC may cause impact on both GSC and RSC outputs. In Option1 the supplementary control is added in the GSC reactive power/voltage control loop for the d-axis to modulate the terminal voltage demand as shown in Fig. 3.

Similarly in Option 2 modulation is through the dc-link voltage reference modulation. The dotted box and line show the SSR damping controller and the injection point. Modulation of the dc-link voltage reference is expected to cause more oscillations on the real power exchange through the dc-link and the electromagnetic torque.

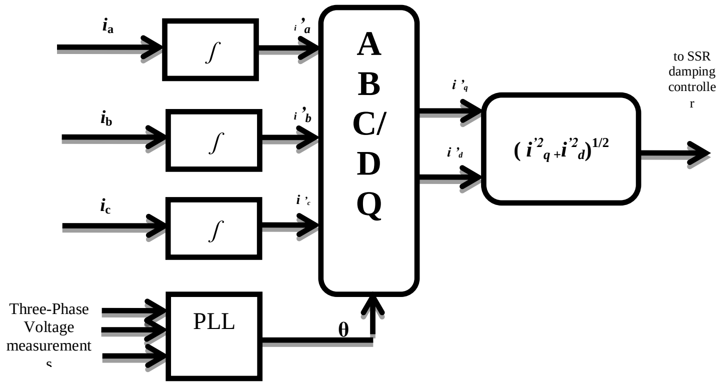

Fig. 4 Estimation of capacitor voltage V_c through three phase current measurement

Therefore, the capacitor voltage can be estimated through the local current measurements. The relationship between the instantaneous current through the line and the instantaneous voltage across the capacitor is given by

$$C\,(dV_{C,P}/dt)=i_p, \text{ where } p = a, b, c$$

The following Fig. 4 presents the estimation diagram of obtaining the estimated voltage magnitude from the a,b,c instantaneous current measurements. Three integral units will be used to obtain another set of signals i_a', i_b' and i_c'. These signals are proportional to the instantaneous capacitor voltage. Through a,b,c to dq reference frame transformation, three-phase balanced variables can be transformed into two dc variables. The fundamental component phasor magnitude can then be computed from the two dc variables.

III. COMPARISON OF CONTROL INPUT SIGNALS

The unique feature of SSR phenomena in wind farms interfaced series compensated network is that induction generator effect due to the network resonant oscillatory mode is the major cause of SSR. Torsional interactions in wind farms are rare because the torsional modes have a low frequency due to the low shaft stiffness of wind turbine drive trains [10].

The rotor speed is used in SSR mitigation control [2], [4].Since it is the network mode that is of the utmost concern, measurements closely related to such mode should be chosen as control signals. Both the line current magnitude and the voltage across the series compensation are chosen.

IV. FUZZY LOGIC CONTROLLER

In a fuzzy logic controller, the control action is determined from the evaluation of a set of simple linguistic rules. The development of the rules requires a thorough understanding of the process to be controlled, but it does not require a mathematical model of the system.

A fuzzy inference system (or fuzzy system) basically consists of a formulation of the mapping from a given input set to an output set using fuzzy logic. This mapping process provides the basis from which the inference or conclusion can be made. A fuzzy inference process consists of the following steps:

- Step 1: Fuzzification of input variables
- Step 2: Application of fuzzy operator (AND, OR, NOT) in the IF (antecedent) part of the rule
- Step 3: Implication from the antecedent to the consequent (THEN part of the rules)
- Step 4: Aggregation of the consequents across the rules
- Step 5: Defuzzification

The crisp inputs are converted to linguistic variables in fuzzification based on membership function (MF). An MF is a curve that defines how the values of a fuzzy variable in a certain domain are mapped to a membership value μ (or degree of membership) between 0 and 1. A membership function can have different shapes; the simplest and most commonly used MF is the triangular-type, which can be symmetrical or asymmetrical in shape. A trapezoidal MF has the shape of a truncated triangle.

The basic properties of Boolean logic are also valid for Fuzzy logic. Once the inputs have been fuzzified, we know the degree to which each part of the antecedent of a rule has been satisfied. Based on the rule, OR or AND operation on the fuzzy variables is done. The implication step helps to evaluate the consequent part of a rule. There are a number of implication methods in the literature, out of which Mamdani and TS types are frequently used. Mamdani proposed this method which is the most commonly used implication method. In this, the output is truncated at the value based on degree of membership to give the fuzzy output. Takagai-Sugeno-Kang method of implication is different from Mamdani in a way that, the output MFs is only constants or have linear relations with the inputs.

The result of the implication and aggregation steps is the fuzzy output which is the union of all the outputs of individual rules that are validated or "fired". Conversion of this fuzzy output to crisp output is defines as defuzzification. There are many methods of defuzzification out of which Center of Area (COA) and Height method are frequently used. In the COA method (often called the center of gravity method) of defuzzification, the crisp output of particular variable Z is taken to be the geometric center of the output fuzzy value $\mu_{out}(Z)$ area, where this area is formed by taking the union of all contributions of rules whose degree of fulfillment is greater than zero. In height method of defuzzification, the COA method is simplified to consider the height of the each contributing MF at the mid-point of the base.

Here in this scheme, the error ***e*** and change of error ***Ce*** are used as numerical variables from the real system. To convert these numerical variables into linguistic variables, the following seven fuzzy levels or sets are chosen as: NB (negative big), NM (negative medium), NS (negative small), ZE (zero), PS (positive small), PM (positive medium), and PB (positive big).

The fuzzy controller is characterized as follows:

- Seven fuzzy sets for each input and output.
- Triangular membership functions for simplicity.
- Fuzzification using continuous universe of discourse.
- Implication using Mamdani's 'min' operator.
- Defuzzification using the 'height' method.

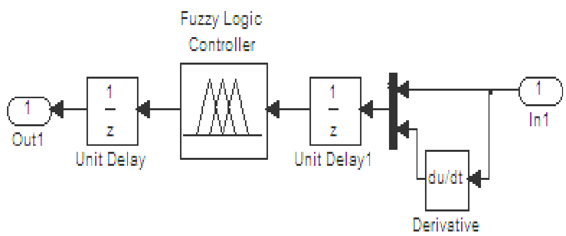

Fig.5 Simulink block diagram for Fuzzy logic Controller

Table1 The rule bases used for the Fuzzy logic controller.

	PL	PM	PS	ZE	NS	NM	NL
PL	**PL**	**PL**	**PL**	**PL**	**PM**	**PS**	**ZE**
PM	**PL**	**PL**	**PL**	**PM**	**PS**	**ZE**	**NS**
PS	**PL**	**PL**	**PM**	**PS**	**ZE**	**NS**	**NM**
ZE	**PL**	**PM**	**PS**	**ZE**	**NS**	**NM**	**NL**
NS	**PM**	**PS**	**ZE**	**NS**	**NM**	**NL**	**NL**
NM	**PS**	**ZE**	**NS**	**NM**	**NL**	**NL**	**NL**
NL	**ZE**	**NS**	**NM**	**NL**	**NL**	**NL**	**NL**

V. SIMULATION

The study system based on the IEEE first benchmark model for SSR studies are shown in Fig. 1 is simulated using MATLAB/SIMULINK. The dynamic responses of the system without SSR damping controller and with SSR damping controller based on PI and fuzzy logic controller based are plotted. The major contributions of the paper are 1) investigation of the potential of wind farm converters for SSR mitigation and 2) identification of an effective control signal for mitigating SSR using fuzzy logic controllers.

Case 1) Without SSR damping controller

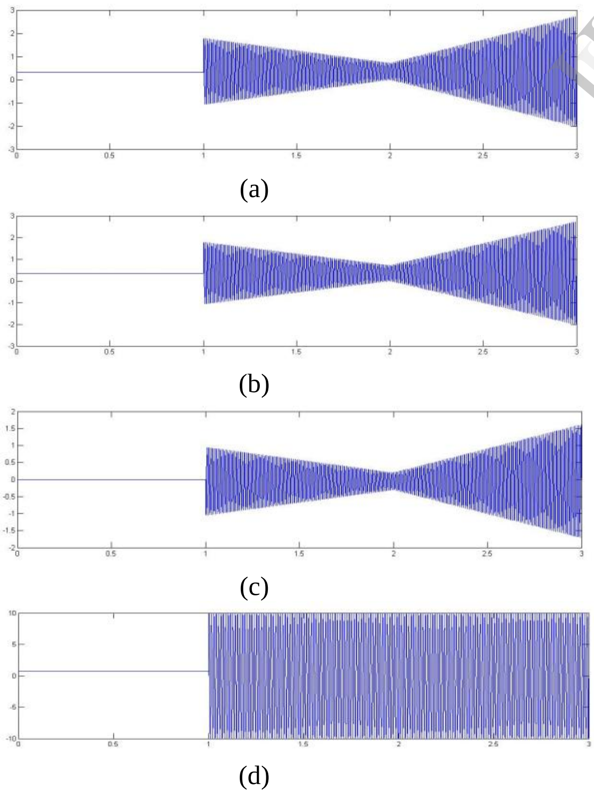

Fig.6 Dynamic responses (a) line current I_{line} , (b) DFIG output power P (c) DFIG exporting reactive power Q , (d) rotor speed W_r .

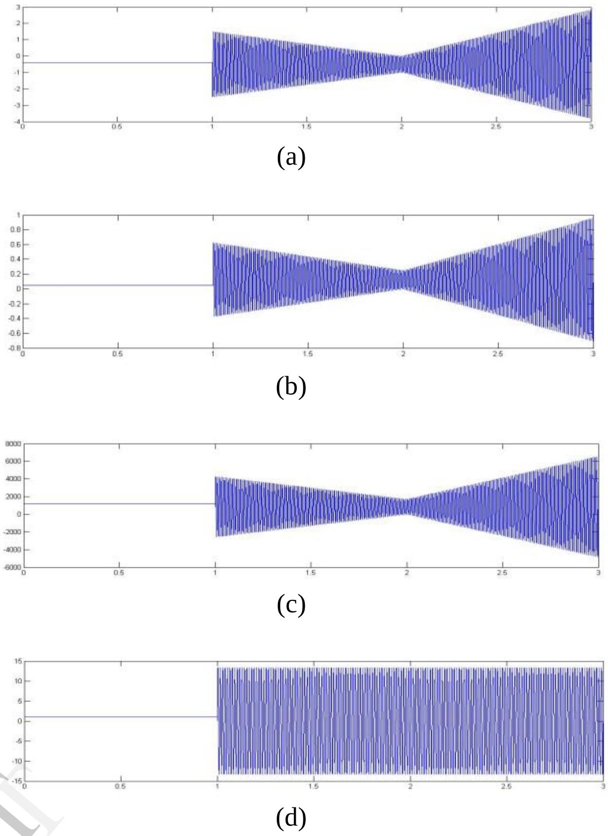

Fig. 7 Dynamic response (a)electromagnetic torque T_e (b) capacitor voltage V_c, (c) dclink voltge V_{dc} (d) terminal voltage V_t .

The increase of power transfer capability of long transmission lines can be achieved by increasing Series compensation level. However, series-compensated transmission lines connected to turbogenerators can result in subsynchronous resonance (SSR), leading to adverse torsional interactions.

In this study shows that when wind speed is 7 m/s, the system can suffer SSR instability when the compensation level reaches 75% due to IGE. In the simulation study, initially, the compensation level is set at 50%. At t = 1 s, the compensation level changes to 75%.

Figs.6 and 7 shows that the dynamic responses line current I_{line} , DFIG output power P, DFIG exporting reactive power Q, rotor speed W_r, electromagnetic torque T_e , capacitor voltage V_c, dclink voltge V_{dc}, terminal voltage V_t of the system without SSR damping controller. From these Figs. it can be observed that the system without damping control becomes unstable when the series compensation level increases to 75%. In rotor speed W_r there exist high oscillations in the waveform because of more torsional interactions.

The dynamic responses of line current I_{line} , DFIG output power P, DFIG exporting reactive power Q , rotor speed W_r, electromagnetic torque T_e,dclink voltge V_{dc}c that there exist oscillations in the waveforms are high due to induction generator effect(IGE). In dclink voltgeV_{dc} there exist high oscillation peak value 2.2KV in the waveform because of induction generator effect (IGE).

Case 2) PI controller vs. fuzzy controller

A) A damping controller is implemented with I_{line} as the input signal and V_t as the output signal. The gain of the controller is 10.

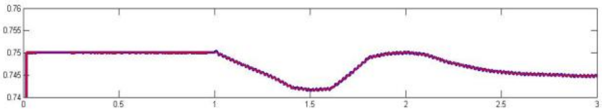

(a)

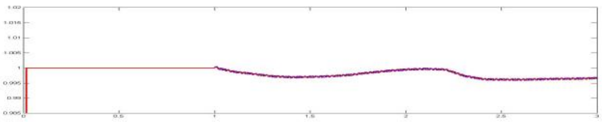

(b)

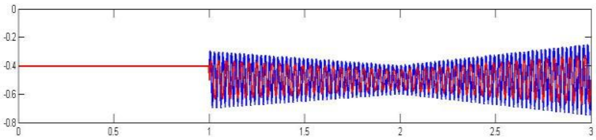

(c)

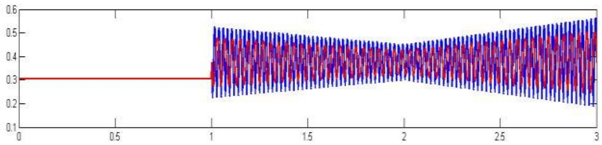

(d)

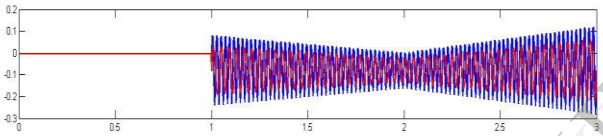

(e)

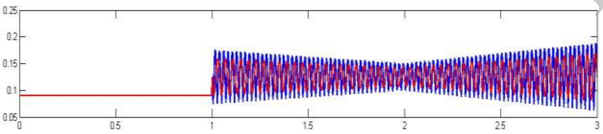

(f)

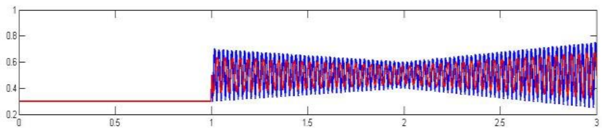

(g)

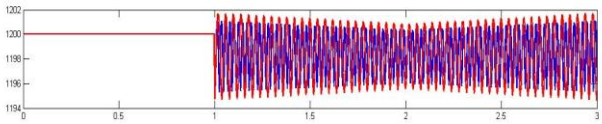

(h)

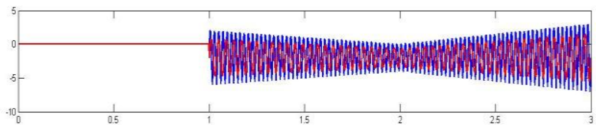

(i)

Fig.8 Dynamic responses (a) rotor speed ω_r ,(b) terminal voltage V_t ,(c) electromagnetic torque T_e , (d) DFIG output power P , (e) DFIG exporting reactive power Q,(f) capacitor voltage V_c , (g) line current I_{line} , (h) dc link voltage V_{dc} , (i) the output of the SSR damping controller ΔV_{ssr} .

In case2 the SSR damping controller is implemented with PI and fuzzy logic controllers with the gains of 10, 30 and 46. The control signals line current magnitude and voltage across the series compensation are chosen. Fig.8 shows that the dynamic responses of rotor speed ω_r , terminal voltage V_t , electromagnetic torque T_e , DFIG output power P, DFIG exporting reactive power Q, capacitor voltage V_c , line current I_{line} , dclink voltage V_{dc} and the output of the SSR damping controller ΔV_{ssr} of the system with PI and fuzzy based SSR damping controller when line current magnitude I_{line} as input control signal and V_t as output control signal. In these waveforms the blue line denotes the system with the SSR damping controller using PI controller while the red line denotes the system with fuzzy logic controller.

Fig.8 shows that the dynamic responses of electromagnetic torque T_e , DFIG output power P, DFIG exporting reactive power Q, capacitor voltage V_c , line current I_{line} , dclink voltage V_{dc} and the output of the SSR damping controller ΔV_{ssr} when gain is 10 respectively slightly reduces SSR damping oscillations except that dc link voltage when the proposed Fuzzy based controller is used. It is observed that the terminal voltage V_t and rotor speed ω_r are having less oscillations compared to without SSR damping controller. In case of without SSR damping controller the output power P the oscillation peak value is 1.75pu, but in PI based SSR damping controller it is reduced to 0.52pu. In Fuzzy controller based SSR damping controller the oscillation peak value further reduced to 0.48pu. Simulation results show that Fuzzy logic controller based decreases the amplitude of SSR damping oscillations.

B) A damping controller is implemented with V_c as the input signal and V_t as the output signal, gain is chosen as 30.

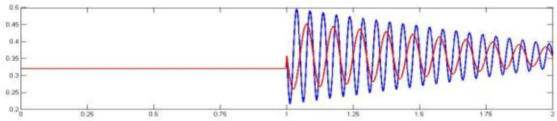

(a)

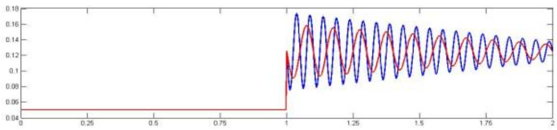

(b)

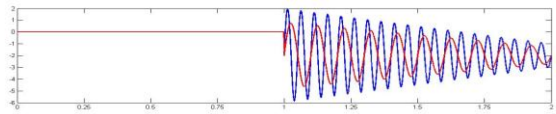

(c)

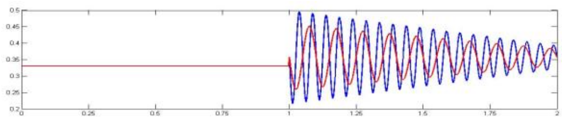

(d)

Fig.9 Dynamic responses (a) line current I_{line} , (b) capacitor voltage V_c ,

(c) the output of the SSR damping controller ΔV_{ssr} . (d) DFIG output powerP, (d) DFIG exporting reactive power Q,

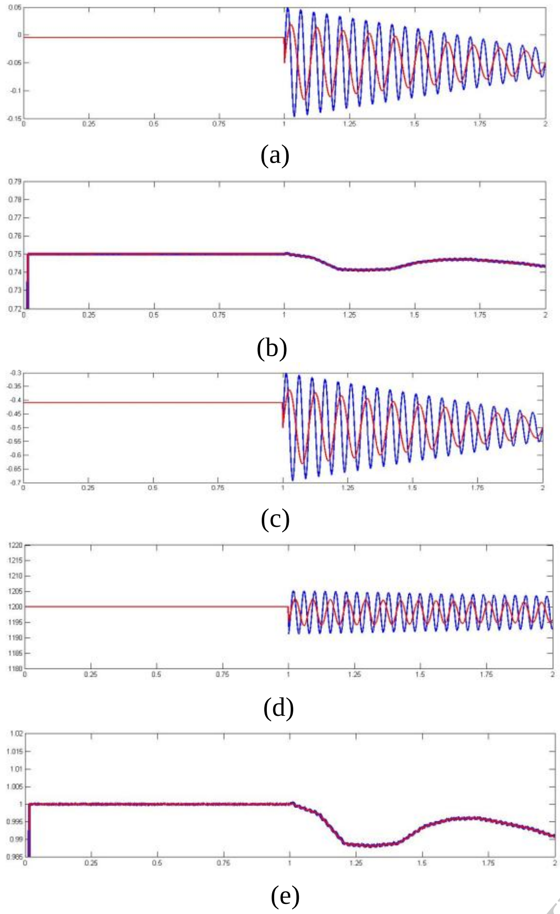

Fig.10 Dynamic responses (a) DFIG exporting reactive power Q, (b) rotor speed ω_r , (c) electromagnetic torque T_e , (d) V_{dc} ,(e) terminal Voltage V_t .

Figs. 9 and 10 shows that the dynamic responses of line current I_{line} , capacitor voltage V_c , DFIG output power P, DFIG exporting reactive power Q, rotor speed, electromagnetic torque T_e , dc link voltage V_{dc} , terminal voltage V_t and the output of the SSR damping controller ΔV_{ssr} of the system with PI vs fuzzy based SSRdamping controller when capacitor voltage V_c as control signal, with gain of 30. In these waveforms the blue line denotes the system with the SSR damping controller using PI controller while the red line denotes the system with fuzzy logic controller.

It is observed that the dynamic responses of terminal voltage V_t and rotor speed ω_r are having less oscillations compared to I_{line} as control signal but these dynamic responses approximately equal when PI and fuzzy based SSR damping controllers are used. In case of PI and fuzzy based SSR damping controller when I_{line} as control signal with gain 10 the output power P oscillation peak values 0.52pu and 0.48pu and these values further reduced to 0.495 and 0.45 when V_c as control signal with gain 30.

Fig.11 shows that the dynamic responses of DFIG output power P, line current I_{line} , DFIG exporting reactive power Q , electromagnetic torque T_e , capacitor voltage V_c , dc link voltage V_{dc} , terminal voltage V_t , wind speed ω_r and the output of the SSR damping controller ΔV_{ssr} of the system with PI and fuzzy based SSRdamping controller when capacitor voltage V_c as input control signal and V_{dc} as output control signal with gain 46.

C) A damping controller is implemented with V_c as the input signal and V_{dc} as the output signal, gain is chosen as 46.

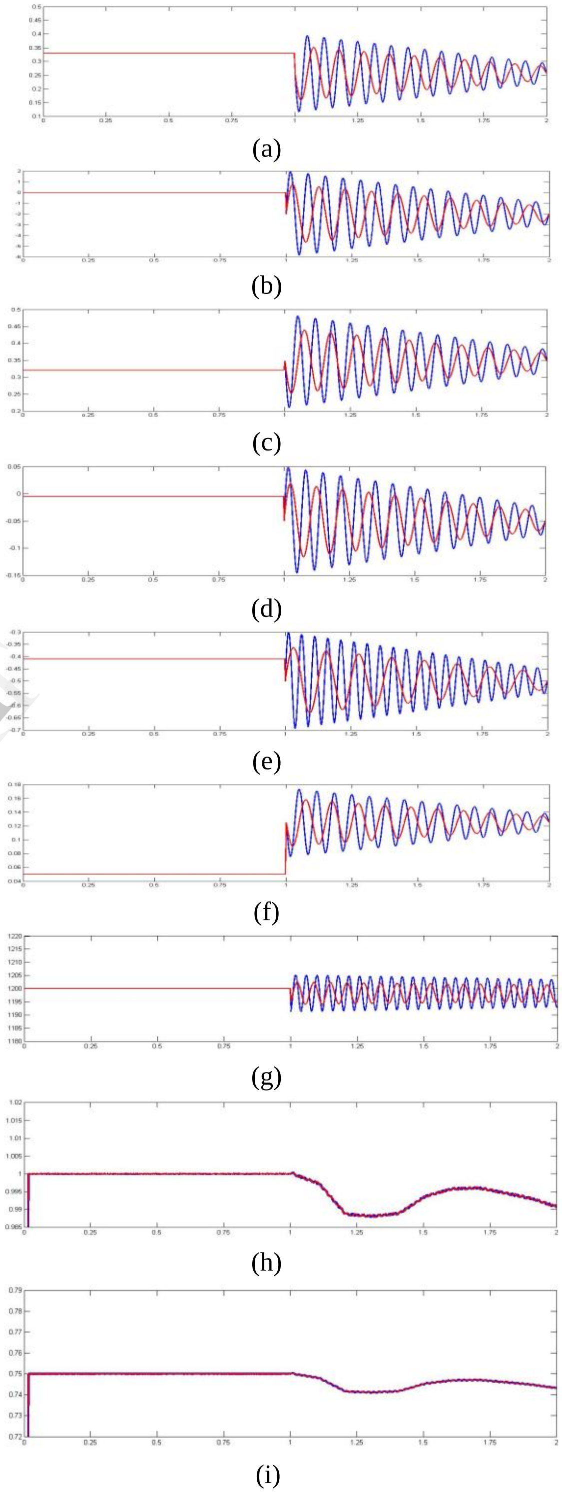

Fig. 11 Dynamic response(a) DFIGoutput powerP , (b) the output of the SSR damping controller ΔV_{ssr} , (c) line current I_{line} , (d) DFIG exporting reactive power Q , (e)electromagnetic torque T_e , (f) capacitor voltage V_c , (g) V_{dc} , (h) terminal voltage V_t , (i) wind speed .

The waveforms in fig.11shows that the blue line denotes the system with the SSR damping controller using PI controller while the red line denotes the system with fuzzy logic controller. It can be observed that the dynamic responses of terminal voltage V_t and rotor speed ω_r are having less oscillations compared to I_{line} as control signal but these dynamic responses approximately equal when PI and fuzzy based SSR damping controllers are used.

In case of PI and fuzzy based SSR damping controller when V_c as control signal with gain 30 the output power P the oscillation peak values 0.495pu and 0.45pu and these values further reduced to 0.395 and 0.351 when V_c as control signal with gain 46. Simulation results show that Fuzzy controller based slightly decreases the amplitude of SSR damping oscillations.

Table2. SSR oscillation (peak) values for I_{line} as control signal with gain 10

Dynamic Response	Without SSR Damping controller	SSR Damping controller with PI	SSR Damping controller with Fuzzy
T_e	1.5	-0.3	-0.36
P_e	1.75	0.52	0.48
Q_e	1	0.08	0.03
V_c	0.6	0.175	0.16
I_{line}	1.8	0.7	0.64
V_{dc}	2200	1201	1201.7
Speed	10	0.7505	0.7503
V_t	12	1.0008	1.0005

Table3. SSR oscillation (peak) values for V_c as control signal with gain 30

Dynamic Response	SSR Damping controller with PI	SSR Damping controller with Fuzzy
T_e	-0.302	-0.362
P_e	0.495	0.45
Q_e	0.05	0.02
V_c	0.174	0.158
I_{line}	0.496	0.45
V_{dc}	1205.3	1202.5
ΔVssr	2	0.75

Table4. SSR oscillation (peak) values for V_c as control signal with gain 46

Dynamic Response	SSR Damping controller with PI	SSR Damping controller with Fuzzy
T_e	-0.301	-0.363
P_e	0.395	0.351
Q_e	0.049	0.018
V_c	0.173	0.158
I_{line}	0.48	0.439
V_{dc}	1205.2	1202.4
ΔVssr	1.95	0.74

The table2 shows that the comparison between without SSR damping controller and PI and fuzzy based SSR damping controller when I_{line} as control signal with gain of 10. From table2 it is observed that the negative peak in the dynamic response of the torque is 1.5pu without SSR damping controller and it is reduced to -0.3pu when PI based SSRdamping controller is implemented. The negative peak in the dynamic response of the torque is further reduced to -0.36pu when fuzzy based SSRdamping controller is used.

The table3 shows that the comparison between PI and fuzzy based SSR damping controller when V_c as control signal with gain of 30. From the table3 it is observed that the negative peak in the dynamic response of the torque is -0.302pu when PI based SSRdamping controller is implemented. The negative peak in the dynamic response of the torque is further reduced to -0.362pu when fuzzy based SSRdamping controller is used.

The table4 shows that the comparison between PI and fuzzy based SSR damping controller when V_c as control signal with gain of 46.From the table4 it is observed that the negative peak in the dynamic response of the torque is -0.301pu when PI based SSRdamping controller is implemented. The negative peak in the dynamic response of the torque is further reduced to -0.363pu when fuzzy based SSRdamping controller is used.

Simulation results show that Fuzzy controller based slightly decreases the amplitude of SSR damping oscillations. Results comparison between conventional PI Controller and the proposed Fuzzy based controller for DFIG indicates that the proposed Fuzzy based controller has less settling time and less overshoot when compared with the conventional PI Controller.

The following observations can also be made from Figs.
1) Both the transmission line current and the voltage across the series capacitor reflect the SSR oscillation well.
2) Though the electromagnetic torque reflects the SSR oscillation, the rotor speed reflects mainly the torsional mode.
3) The terminal voltage shows SSR oscillation due to the damping controller.

Overall, the control signal V_c can effectively damp SSR oscillations. In this paper observed that the capacitor voltage is an effective control signal for SSR mitigation when V_{dc} as output control signal with fuzzy logic controller.

VI. CONCLUSION

In this paper an effective control signal for SSR damping controller is implemented which mitigate both sub synchronous and super synchronous resonance in DFIG. Various simulations are carried out to analyze the performance of the system. Both Proportional Integral (PI) controller based and fuzzy logic controller based are implemented for mitigating SSR in wind farms connected with series compensated transmission network. Auxiliary damping control schemes to modulate either the terminal voltage or the dc-link voltage references of the grid side converter controls are proposed for SSR mitigation. Capacitor voltage is demonstrated to be an effective signal to enhance damping for both SSR and supersynchronous modes. Though it is a remote signal, it can be estimated through local current measurements. The performance of both the controllers has been studied and compared. A model has been developed in MATLAB /SIMULINK and simulated to verify the results. The fuzzy logic controller based SSR damping controller has a better performance compared with PI controller in steady state response and less settling time.

APPENDIX

The parameters of the DFIG and study system are shown in Tables 5 to 7

TABLE 5
Parameters of a Single 2-Mw DFIG and the Aggregated DFIG in network system

Rated power	2 MW	100 MW
Rated voltage	690 V	690 V
X_{ls}	0.09231 pu	0.09231 pu
X_m	3.95279 pu	3.95279 pu
X_{lr}	0.09955 pu	0.09955 pu
R_s	0.00488 pu	0.00488 pu
R_r	0.00549 pu	0.00549 pu
H	3.5 s	3.5 s
X_{tg}	0.3 pu (0.189 mH)	0.3 pu (0.189/5 mH)
DC link capacitor C	14000 Mf	50×14000µF
DC link rated voltage	1200 V	1200 V

TABLE 6
Parameters of the network system

Transformer ratio	690V/161KV
Transformer X_T	0.14 pu
Base MVA	100 MVA
R_L	0.02 pu (5.1842Ω)
X_L	0.5 pu (129.605Ω)
X_C at 50% compensation level	64.8Ω
Series compensation C	40µF
Line length	154 mile

TABLE 7
Parameters of the Control Loops in A DFIG

T_{Te}	0.025	T_{Qs}	0.05
T_{iq}	0.0025	T_{id}	0.005
K_{Te}	0.1	K_{Qs}	0.1
K_{iq}	0.0	K_{id}	0.0
K_{p3}	1	K_{i3}	100
K_{p4}	0.1	K_{i4}	0.05

REFERENCES

[1] Lingling Fan, and Zhixin Miao,"Mitigating SSR Using DFIG-Based Wind Generation', IEEE Trans. Sustain Energy., vol. 3, no. 3, pp. 349–358 July 2012
[2] R. K. Varma, S. Auddy, and Y. Semsedini, "Mitigation of sub synchronous resonance in a series-compensated wind farm using FACTS controllers," IEEE Trans. Power Del., vol. 23, no. 3, pp. 1645–1654,Jul. 2008.
[3] A. Ostadi, A. Yazdani, and R. Varma, "Modeling and stability analysis of a DFIG-based wind-power generator interfaced with a series-compensated line," IEEE Trans. Power Del., vol. 24, no. 3, pp. 1504–1514,Jul. 2009.
[4] M. S. El-Moursi, B. Bak-Jensen, and M. H. Abdel-Rahman, "Novel STATCOM controller for mitigating SSR and damping power system oscillations in a series compensated wind park," IEEE Trans. Power Electron., vol. 25, no. 2, pp. 429–441, Feb. 2010.
[5] A. Tapia, G. Tapia, J. X. Ostolaza, and J. R. Saenz, "Modeling and control of a wind turbine driven doubly fed induction generator," IEEE Trans. Energy Convers., vol. 18, no. 2, pp. 194–204, Jun. 2003.
[6] L. Xu and Y. Wang, "Dynamic modeling and control of DFIG-based wind turbines under unbalanced network conditions," IEEE Trans. Power Syst., vol. 22, no. 1, pp. 314–323, Feb. 2007.
[7] F. M. Hughes, O. Anaya-Lara, N. Jenkins, and G. Strbac, "A power system stabilizer for DFIG-based wind generation," IEEE Trans. Power Syst., vol. 21, no. 2, pp. 763–772, May 2006.
[8] Z. Miao, L. Fan, D. Osborn, and S. Yuvarajan, "Control of DFIG based wind generation to improve inter area oscillation damping," IEEE Trans. Energy Convers., vol. 24, no. 2, pp. 415–422, Jun. 2009.
[9] L. Fan, R. Kavasseri, Z. Miao, and C. Zhu, "Modeling of DFIG-based wind farms for SSR analysis," IEEE Trans. Power Del., vol. 25, no. 4,pp. 2073–2082, Oct. 2010.
[10] F. Mei and B. Pal, "Modal analysis of grid-connected doubly fed induction generators," IEEE Trans. Energy Convers., vol. 22, no. 3, pp.728–736, Aug. 2007.
[11] C. Zhu, L. Fan, and M. Hu, "Control and analysis of DFIG-based wind turbines in a series compensated network for SSR damping," in Proc. IEEE Power & Energy General Meeting, Minneapolis, MN, Jul. 2010.
[12] "First benchmark model for computer simulation of sub synchronous resonance," IEEE Trans. Power App. Syst., vol. 96, no. 5, pp.1565–1672, Sep./Oct. 1977, IEEE Committee Report.
[13] L. M. Fernandez, F. Jurado, and J. R. Saenz, "Aggregated dynamic model for wind farms with doubly fed induction generator wind turbines," Renew. Energy, vol. 33, pp. 129–140, 2008.
[14] J. T. Bialasiewics and E. Muljadi, The Wind Farm Aggregation Impacton Power Quality, National Renewable Energy Laboratory Report, Nov. 2006 [Online]. Available:http://www.nrel.gov/wind/pdfs/39870.
[15] E.Muljadi and B. Parsons, "Comparing single and multiple turbine representations in a wind farm simulation," in Proc. Eur. Wind Energy Conf., Athens, Greece, 2006.
[16] M. Poller and S. Acchilles, "Aggregated wind park models for analyzing power system dynamics," in Proc. 4th Int. Workshop on Large-Scale Integration of Wind Power and Transmission Networks for Offshore Wind Farms, Billund, Denmark, 2003.
[17] F.Mei and B. C. Pal, "Modelling of dobuly-fed induction generator for power system stability study," in Proc. IEEE Power & Energy General Meeting 2008, Pittsburgh, PA, Jul. 2008.
[18] D.Maksimovic, A.Stankovic, V. Thottuvelil, and G. Verghese, "Modeling and simulation of power electronic converters," Proc. IEEE, vol.89, no. 6, pp. 898–912, Jun. 2001.
[19] Mitigation of SSR and LFO with a TCSC based-conventional damping controller optimized by the PSO algorithm and a fuzzy logic controller Hasan GHAHRAMANI, Akbar LAK, Murtaza FARSADI, Hossein HOSSEINI Department of Electrical Engineering, University of Urmia, Urmia, Ira
[20] H. He,\Fuzzy modeling and fuzzy control [book review]", Computational Intelligence Magazine, IEEE, Vol. 3, pp. 8{10, 2008.
[21] H.J. Zimermann, Fuzzy Set Theory and its Applications, 3rd Edition, The Netherlands, Kluwer Academic Publishers, 1996.